Cao, C., Gao, X., & Conn, A. (2019). Contactless coupling of dielectric elastomer membranes with magnetic repulsion. In Y. Bar-Cohen (Ed.), *Electroactive Polymer Actuators and Devices (EAPAD) XXI* [109660P] (Proceedings of SPIE; Vol. 10966). Society of Photo-Optical Instrumentation Engineers (SPIE). https://doi.org/10.1117/12.2522127

Contactless coupling of dielectric elastomer membranes with magnetic repulsion

Chongjing Cao[a,c], Xing Gao*[b,c], Andrew T. Conn[b,c]
[a]Dept. of Aerospace Engineering, University of Bristol, Bristol BS8 1TR, UK;
[b]Dept. of Mechanical Engineering, University of Bristol, Bristol BS8 1TR, UK;
[c]Bristol Robotics Laboratory, Bristol BS16 1QY, UK

ABSTRACT

Dielectric elastomer (DE) actuators such as conventional double cone configurations have demonstrated that coupled DE membranes can be rigidly-coupled to execute antagonistic out-of-plane actuation. This paper presents experimental analysis of the compliant coupling in the emerging magnetically-coupled DE actuator (MCDEA) design, which exploits contactless magnetic repulsion to create a frictionless coupling between DE membranes. The compliance of this coupling enables the advantage of having two different actuation modes: antagonistic reciprocation and bi-directional expansion. However, since this compliance adds an additional degree-of-freedom, it increases the complexity of the actuator's dynamics because the coupling distance can exhibit oscillatory behavior that is distinct from each of the actuator's output oscillations in terms of phase difference and frequency. In this work, the relationship between DEA membrane stiffness and required magnetic force is experimentally analyzed before we present an investigation into the phase space of the compliant coupling and its relationship with the stroke amplitude. It is shown that the fundamental frequency of the MCDEA's output stroke (46.1 Hz) corresponds to a super-harmonic frequency of the magnetic coupling that is double that of the output. The fundamental frequency of the coupling (87.6 Hz) is found to correspond to a second resonant peak in the MCDEA's output with a much lower amplitude than at 46.1 Hz. This suggests that the dynamics can be exploited by controlling the excitation frequency for unidirectional push/pull or bidirectional expansion/contraction actuation, which creates potential for new compliant DE actuator and generator designs.

Keywords: Dielectric elastomer actuator, compliant coupling, magnetic biasing force, antagonistic actuation, resonance.

1. INTRODUCTION

Dielectric elastomer actuators (DEAs) are formed from thin elastomeric films coated with compliant electrodes and they exhibit attractive characteristics such as large actuation strains and high energy densities [1]. DEAs are driven by large electric fields that generate a Maxwell pressure which induces large biaxial planar expansion and transverse compression. Out-of-plane biasing mechanisms can help to maximize the linear actuation stroke output from this biaxial expansion, and these include the use of a rod [2, 3], spring [4, 5], deadweight [6, 7] or magnetic force [8, 9] to deform the DEA membrane into a protruding conical shape. Out-of-plane biasing can also be achieved using an antagonistic DEA configuration, as demonstrated by Artificial Muscle Incorporated's Universal Muscle Actuator [10], which connected two offset membranes via a co-axial central disk to form a recessed conical shape. Coupling DEA membranes in an antagonistic configuration draws clear parallels to the skeletal muscle architectures in nature and similarly generates benefits such as maximizing stroke and offering dual capabilities for either bi-directional push/pull actuation (when each membrane is driven out-of-phase) or increased holding force (when the membranes are activated in-phase and in tension against each other) [11]. DEAs with antagonistically-coupled membranes have been exploited for numerous applications including bistable structures [12] and bio-inspired robotics such as manipulators [13] and walking [14], crawling [15] and flapping wing [16] robots.

DEAs with antagonistically-coupled out-of-plane membranes have typically relied on either a rigid [2, 3, 11] or hydrostatic [17] coupling between each membrane. Rigid coupling using a rod [2, 3] or disk [11] creates a double cone configuration while hydrostatic coupling utilizes fluid pressure from an internally sealed volume to deform each DEA membrane into a hemispherical diaphragm [17]. If an incompressible fluid is used in the hydrostatically-coupled configuration, then each DEA diaphragm is, in effect, also rigidly coupled. Rigid coupling between membranes can be

* xing.gao@bristol.ac.uk

advantageous for ease of control, since only one membrane's position is needed to know the kinematic state of the actuator, but the membrane displacements are limited to a phase difference of only 180° during periodic actuation cycles.

A compliant coupling between DEA membranes creates opportunities for both antagonistic push/pull actuation as well as in-phase expansion/contraction, where the coupling is extended or compressed by synchronized membrane activation. In this work, we analyze the dynamics of the compliant coupling between membranes in our recently published magnetically-coupled DEA (MCDEA) design [18]. The double cone MCDEA exploits a magnetic repulsion force via embedded permanent magnets to deform a pair of membranes out-of-plane. Compliant, out-of-plane biasing may also be achieved using a spring (analogous to the spring roll DEA design [19]) but this is not contactless unlike magnetic repulsion and a recent study on individual out-of-plane DEA membranes found that a permanent magnet biasing force could increase the actuation stroke in comparison to a spring [8]. The hydrostatically-coupled DEA configuration may also exhibit compliant coupling if a compressible fluid is used, but since it generates volumetric expansion through DEA diaphragms, whereas the MCDEA generates a linear stroke via a rigid end effector, they are not directly comparable.

In this work, we present a new analysis of the dynamics of the compliant coupling in the double cone MCDEA design. First, an overview of the MCDEA's design and principle of operation is given (section 2), before the methods and materials for its fabrication and testing are described (section 3). Quasi-static experimental characterization of the force-displacement responses of a single DEA membrane and the coupled permanent magnets are presented in section 4.1, before the frequency-dependent response of the MCDEA's compliant coupling is analyzed in depth in section 4.2. In contrast to previous analysis of the MCDEA in [18], here we investigate the specific dynamics and phase space of the compliant coupling and its relationship with the actuator's stroke amplitude.

2. MAGNETICALLY-COUPLED DIELECTRIC ELASTOMER

The magnetically-coupled DEA (MCDEA) consists of two circular DEA membranes which each have a permanent magnet attached in their center. The membranes are configured in parallel with the magnets co-axially aligned and oriented so that their poles create a linear magnetic repulsion force, F_{mag}, that biases the membranes out-of-plane (as shown in Figure 1) [18]. The out-of-plane biasing creates a conical shape, which results in the membranes having a higher radial principal stretch, λ_1, relative to the circumferential principal stretch, λ_2 (after [4, 20]).

The coupling in the MCDEA is due to the force equilibrium between the out-of-plane tension force exerted on the magnets by each membrane and F_{mag}. Since each membrane's tension, and hence the reaction force on the magnet, is subject to voltage-induced modulation, the distance between the magnets is not restricted and may be controlled. Since this coupling is compliant and the two DEA membranes are arranged antagonistically, it was shown in [18] that changing the phase difference between each membrane's applied voltage could generate distinct actuation modes. If the membranes are excited with driving signals that are 180° out-of-phase, then a bi-directional linear stroke is observed. If equal voltages are applied to the membranes in-phase (0°), then the reaction forces exerted on both magnets are reduced and the coupling distance, *s*, increases (i.e. the MCDEA expands outwards). The additional linear degree-of-freedom (DOF) between the magnets adds complexity to the MCDEA's dynamics, since the coupling distance, *s*, can exhibit oscillatory behavior that is distinct from each of the magnet's oscillations in terms of phase difference and frequency, even when only one DEA membrane is actuated. Experimental results of these dynamics are analyzed in section 4.2.

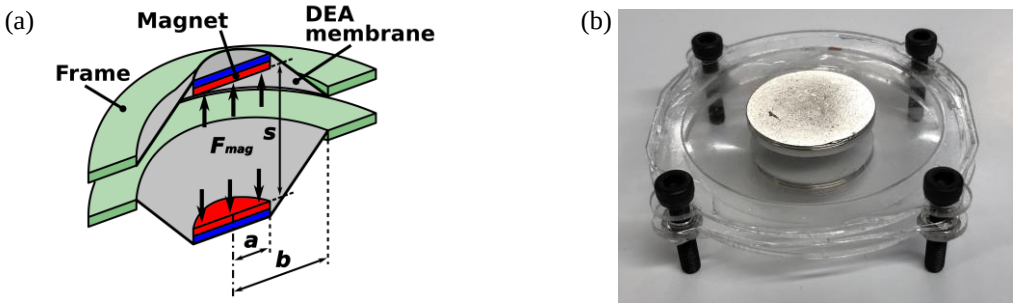

Figure 1. (a) Cross-sectional assembly view of the MCDEA showing magnetic repulsion force, F_{mag}, magnet radius, *a*, membrane radius, *b*, and coupling distance, *s*. (b) An assembled MCDEA prototype shown without electrodes for clarity.

3. MATERIALS AND METHODS

3.1 MCDEA fabrication

The fabrication process described here follows that presented in [18]. The MCDEA was fabricated using two 100 μm thick silicone elastomer membranes (Elastosil, Wacker Chemie AG), which were biaxially pre-stretched 1.2×1.2 before being bonded to separate circular acrylic frames (40 mm inner diameter) using silicone transfer tape (ARclear 93495, Adhesives Research). A disc-shaped Neodymium magnet (First4Magnets) was bonded to the center of each membrane using the same silicone transfer tape. Each magnet has a rated pull force of 0.28 kg and maximum energy product of 318 - 342 kJ/m^3 with a 15 mm diameter and 0.5 mm thickness. After each magnet was bonded, electrodes were manually applied to each side of the membrane using carbon grease (MG Chemicals). The magnets were oriented so that the same pole on each magnet was on the bonded magnet-membrane interface. This ensured that a magnetic repulsion force was generated between the membranes, so that they deformed out-of-plane into a double cone configuration when their circular frames were bolted together (as shown in Figure 1b).

3.2 Experimental method

Two sets of experiments were conducted to (i) characterize the relative stiffness of the elastomer membrane and magnetic repulsion force and (ii) analyze the dynamics of the compliant coupling in the MCDEA. The first of these tests measured the quasi-static force-displacement responses of a single DEA membrane and the coupled magnetic repulsion and the second tests considered the frequency-dependent response of the complete MCDEA, with a focus on the dynamics of the compliant coupling.

For the quasi-static tests, a single DEA membrane was fabricated following the MCDEA fabrication procedure described in section 3.1, except that only one circular frame with membrane and bonded magnet was produced. The DEA membrane's frame was fixed in place while the magnet was displaced by a passive rod driven by a linear actuator (X-LSQ150B-E01, Zaber Technologies Inc.), as shown in Figure 2a. The rod was connected in series to a load cell (NO.1004, Tedea) so that the reaction force from the silicone elastomer membrane could be measured. The protruding rod was translated at a constant rate of only 0.01 mm/s to ensure the viscoelastic contributions to the response of the were negligible. The displacement of the magnet on the DEA membrane was measured using a laser displacement sensor (LK-G152 and LKGD500, Keyence). The force-displacement response was conducted while the DEA membrane was passive and when a voltage of 4170 V was applied by a high voltage amplifier (Ultravolt, 5HV23-BP1), which corresponds to a nominal electric field, E_n, of 60 V/μm. E_n was estimated using the biaxial pre-stretch, λ_p, value of 1.2 and the incompressibility assumption ($\lambda_1\lambda_2\lambda_3 = 1$).

The magnetic repulsion force was measured with a similar set-up using the linear actuator, load cell and laser displacement sensor. One magnet was fixed in place while the other was displaced by the linear actuator with the load cell connected in series so that the force-displacement relationship between F_{mag} and s could be measured. In all tests, data was collected using a DAQ device (National Instruments, BNC-2111) with MATLAB (Mathworks).

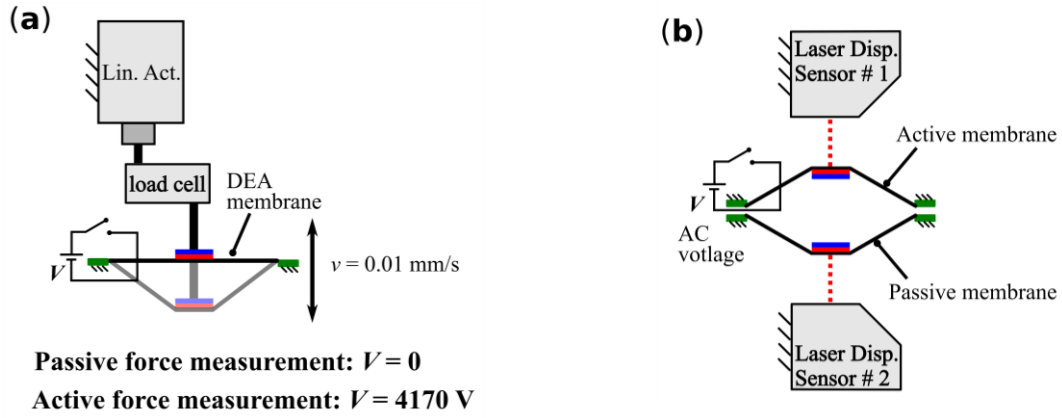

Figure 2. Experimental set-up: (a) measurement of quasi-static membrane stiffness with passive and active DEA states; (b) measurement of dynamic oscillations under excitement from an AC voltage signal applied to one DEA membrane.

The dynamic actuation tests of the MCDEA required no externally applied forces and hence the protruding rod, load cell and linear actuator from the quasi-static tests were not included. Two laser displacement sensors (same model as above) where used to measure the displacement of both magnets and hence determine changes in the compliant coupling distance, *s* (as shown in Figure 2b). In all dynamic tests, one membrane in the MCDEA was activated with a sinusoidal driving voltage while the other remained passive. The driving signal's excitation frequency, Ω, was swept from 1 to 200 Hz in increments of 0.1 Hz. Each frequency increment was maintained for 10 cycles to ensure a steady-state response was attained. The peak voltage in the sinusoidal signal was 4170 V, which corresponds to a nominal electric field, E_n, of 60 V/μm.

4. EXPERIMENTAL RESULTS

4.1 Quasi-static characterization

The quasi-static force-displacement of the DEA membrane demonstrated a relatively linear response in its passive state, as shown in Figure 3a. Minimal hysteresis was evident in the response, which is expected considering the typically low viscoelasticity of silicone elastomers. With a constant voltage of 4170 V applied, the DEA membrane's stiffness relaxed, and it continued to exhibit negligible hysteresis. The magnetic repulsion force is plotted against the distance between the magnets, *s*, in Figure 3b. It exhibits a more non-linear force-displacement curve relative to the DEA membrane and has an inverse stiffness since it is a repulsive magnetic coupling. As the dashed lines across Figure 3 indicate, when the DEA membranes and magnets are balanced with no actuation voltage, the force is 305 mN, and when a voltage of 4170 V is applied to one membrane, the force reduces to 255 mN. This method of characterizing the relative stiffness of the DEA membranes and magnetic repulsion can enable the design of MCDEAs with different membrane stiffnesses (perhaps due to a different elastomer modulus or multi-layered stacking), since the corresponding magnetic repulsion force can be easily determined as shown here.

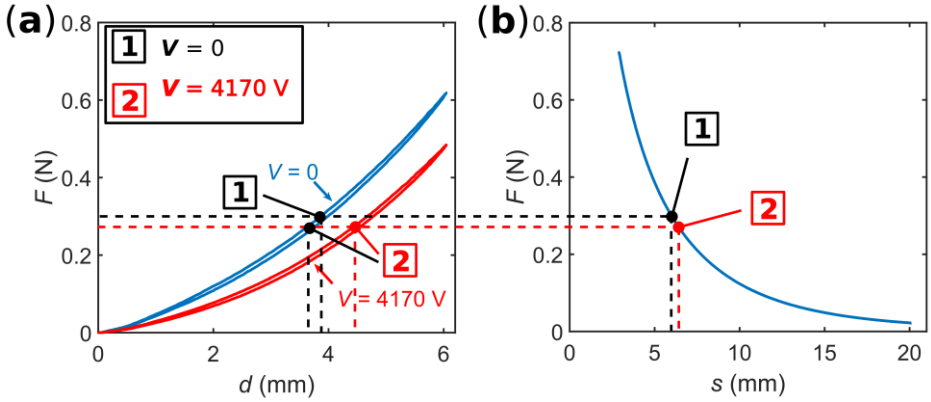

Figure 3. Force-displacement responses: (a) single DEA membrane in passive and active states; (b) magnetic repulsion force. The dashed lines indicate where balanced membrane-magnet coupling states exist in the passive and active states (data reproduced from [18]).

4.2 Dynamic response of compliantly coupled actuator

Characterizing the relationship between the fundamental frequency of the magnetic coupling's oscillation relative to the fundamental frequency of the MCDEA's output oscillation is key towards understanding the effect of the coupling's compliance on the actuator dynamics and stability. In all cases, the fundamental frequency is defined as the frequency with the largest magnitude in a discrete Fourier transform.

Figure 4 plots the fundamental frequency, ω, of both the MCDEA's output stroke (Figure 4a) and coupling distance, *s*, (Figure 4b) against the excitation frequency, Ω (described in section 3.2). Figures 4c and 4d show the corresponding

frequency response of stroke amplitude and s respectively. It can be seen in Figure 4c that the MCDEA has a super-harmonic peak amplitude of 1.77 mm at Ω = 23.5 Hz, which corresponds to the output stroke oscillating at twice the frequency of the applied voltage ($\omega = 2\Omega$), as shown in Figure 4a. The next peak in Figure 4c, at Ω = 46.1 Hz, is a resonant peak where the excitation and fundamental response frequencies are matched ($\omega = \Omega$). This frequency generates the largest stroke amplitude of 4.06 mm, which is equivalent to a strain of 10% relative to the membrane diameter. The third peak in Figure 4c, at Ω = 87.6 Hz, is another resonant frequency ($\omega = \Omega$), but it exhibits a much smaller amplitude of 1.27 mm due the oscillation of the compliant coupling (described below).

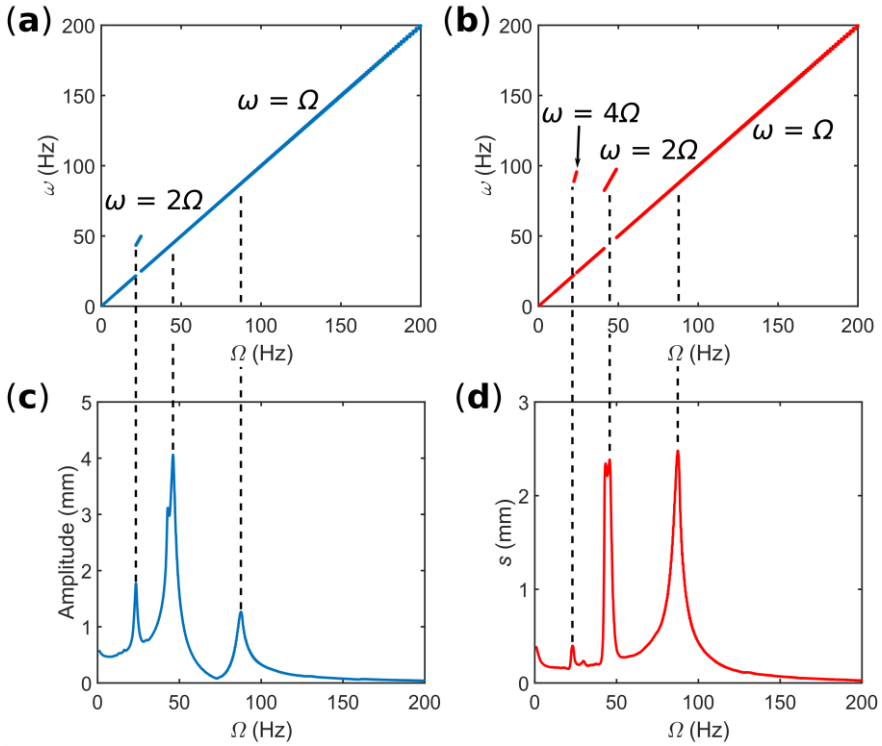

Figure 4. Frequency response of the MCDEA with one active membrane driven at excitation frequency, Ω: (a) fundamental frequency, ω, of the driven membrane's magnet against Ω; (b) fundamental frequency, ω, of coupling distance, s, against Ω; (c) oscillation amplitude of the driven membrane's magnet against Ω; (d) oscillation amplitude of s against the Ω (data in Figure 4c reproduced from [18]).

The frequency response of the MCDEA output only gives a superficial understanding of the actuator's dynamics, as the additional DOF introduced by the compliant coupling contributes underlying characteristics to the response. Complementary to the frequency-dependent response of the compliant coupling in Figures 4b and 4d are the time-dependent periodic oscillations of s in Figures 5a, 5c and 5e and phase portraits in Figures 5b, 5d and 5f.

At an excitation frequency of 23.5 Hz, the MCDEA output exhibits a super-harmonic response ($\omega = 2\Omega$) and small stroke amplitude (1.77 mm), while the compliant coupling has a very small amplitude of s (Figure 4d) and its super-harmonic fundamental frequency, ω, is much larger than the excitation frequency ($\omega = 4\Omega$). The relatively weak stability of the coupling's response at this frequency is more clearly shown in the phase portrait (Figure 5b), where the spiraling limit cycle is much less clearly defined than the responses at 46.1 Hz (Figure 5d) and 87.6 Hz (Figure 5f). At the resonant frequency of the MCDEA with the largest stroke amplitude (46.1 Hz, Ω = 4.06 mm), the compliant coupling exhibits a large super-harmonic ($\omega = 2\Omega$) peak amplitude of s = 2.39 mm. At this frequency, the periodic oscillation is a lot more stable than at 23.5 Hz (Figure 5c) and the phase portrait has a clear attractor (Figure 5d). The reason that s cycles periodically with a larger negative (compression) than positive amplitude (expansion) in Figure 5c, is because only one DEA membrane is excited, and this introduces an asymmetry between the driving and return forces.

In the Figure 4d, it can be seen that the MCDEA output's resonant frequency of 87.6 Hz is also the fundamental frequency at which the compliant coupling resonates ($\omega = \Omega$) with the largest amplitude of s = 2.50 mm. It is interesting to note that although this is the only frequency at which the fundamental frequencies of both the MCDEA's output and

compliant coupling match both each other and Ω, this is the lowest stroke amplitude of any of the three peaks in Figure 4c. This is because this resonant frequency is dominated by the magnetic coupling of the two membranes and consequently it is s which is oscillating with a large amplitude. This behavior corresponds to the MCDEA primarily oscillating in an expanding and contracting mode, where s cycles periodically about its passive position (s = 0 mm), as shown in Figure 5e. At this frequency, the compliant coupling exhibits the most stable dynamics, as exemplified by the phase portrait in Figure 5f where there is a very clear limit cycle.

It can be concluded from this analysis, that the dynamics of the compliant coupling in the MCDEA may be exploited for different applications. For example, where a large, reciprocating output stroke is required, the resonant frequency of 46.1 Hz is ideal as this is where the compliant coupling oscillates at a super-harmonic frequency twice that of the excitation frequency. If a large expansion and contraction of the MCDEA is desired, then the resonant frequency of 87.6 Hz is preferable as s oscillates with a large amplitude of 2.50 mm. It is proposed that the resonant frequencies may be tuned to different values by changing the membrane stiffness and magnet strength and this will be investigated in future work.

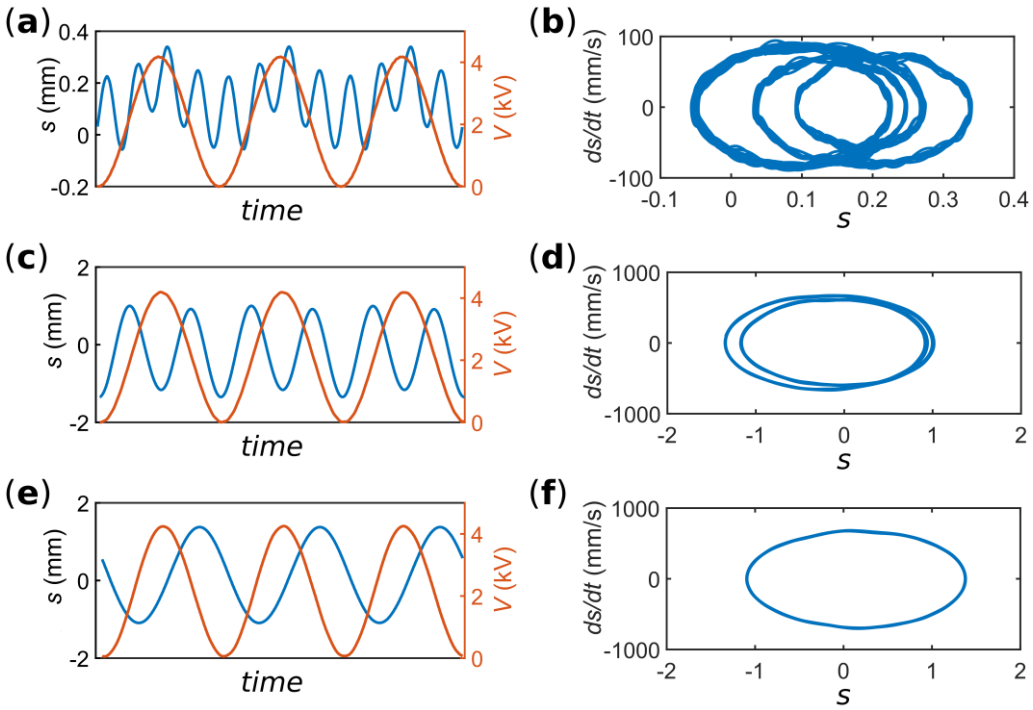

Figure 5. Dynamic response of the compliant coupling distance, s, in the time domain (a,c,e) and phase plane (b,d,f). Responses for three different excitation frequencies, Ω, with corresponding fundamental frequency, ω, of s are shown in: (a,b) Ω = 23.5 Hz and $\omega = 4\Omega$; (c,d) Ω = 46.1 Hz and $\omega = 2\Omega$; (e,f) Ω = 87.6 Hz and $\omega = \Omega$.

5. CONCLUSION

In this work, we have investigated the dynamics associated with the compliant coupling in a double cone MCDEA, which is an emerging linear stroke DEA configuration. The phase space of the compliant coupling was tested with varying excitation frequencies to study the relationship between coupling distance and stroke amplitude. The dynamic results showed that that the fundamental frequency of the MCDEA's output stroke (46.1 Hz) corresponds to a super-harmonic frequency of the magnetic coupling that is double that of the output. The fundamental frequency of the coupling (87.6 Hz) is found to correspond to a second resonant peak in the MCDEA's output with a much lower amplitude than at 46.1 Hz. This suggests that the complex dynamics of the MCDEA can be exploited for different applications by changing the excitation frequency for unidirectional push/pull or bidirectional expansion/contraction actuation.

ACKNOWLEDGEMENTS

C. Cao appreciates the support from the EPSRC Centre for Doctoral Training in Future Autonomous and Robotic Systems (FARSCOPE) at the Bristol Robotics Laboratory. X. Gao and A. Conn acknowledge support from EPSRC grant EP/P025846/1.

REFERENCES

[1] Pelrine, R., Kornbluh, R., Pei, Q. and Joseph, J., "High-speed electically actuated elastomers with strain greater than 100%," *Science*, 287, 836-839 (2000).

[2] Choi, H.R., Jung, K.M., Kwak, J.W., Lee, S.W., Kim, H.M., Jeon, J.W. and Nam, J.D., "Digital polymer motor for robotic applications, " *Proc. IEEE ICRA 2003*, 1857–62, (2003).

[3] Conn, A.T. and Rossiter, J., "Towards holonomic electro-elastomer actuators with six degrees of freedom," *Smart Mater. and Struct.*, 21(3), (2012).

[4] Berselli, G., Vertechy, R., Vassura, G. and Parenti-Castelli, V., "Optimal synthesis of conically shaped dielectric elastomer linear actuators: design methodology and experimental validation, " *IEEE-ASME Trans. Mech.*, 16, 67–79 (2011).

[5] Hodgins, M., Rizzello, G., Naso, D., York, A. and Seelecke, S., "An electro-mechanically coupled model for the dynamic behavior of a dielectric electro-active polymer actuator," *Smart Mater. and Struct.*, 23(10), 104006 (2014).

[6] He, T., Cui, L., Chen, C. and Suo, Z., "Nonlinear deformation analysis of a dielectric elastomer membrane-spring system," *Smart Mater. and Struct.*, 19(8), 085017 (2010)

[7] Hodgins, M., York, A. and Seelecke, S., "Experimental comparison of bias elements for out-of-plane DEAP actuator system," *Smart Mater. and Struct.*, 22(9), 094016 (2013).

[8] Loew, P., Rizzello, G. and Seelecke, S., "A novel biasing mechanism for circular out-of-plane dielectric actuators based on permanent magnets," *Mechatronics*, 56, 48-57 (2018).

[9] Yang, T., Xiao, Y., Zhang, Z., Liang, Y., Li, G., Zhang, M., Li, S., Wong, T.W., Wang, Y., Li, T. and Huang, Z., "A soft artificial muscle driven robot with reinforcement learning," *Scientific Reports*, 8, 14518 (2018).

[10] Bonwit, N., Heim, J., Rosenthal, M., Duncheon, C. and Beavers, A., "Design of commercial applications of EPAM technology, " *Proc. SPIE 6168*, 616805 (2006).

[11] Conn, A.T. and Rossiter, J., "Antagonistic dielectric elastomer actuator for biologically-inspired robotics," *Proc. SPIE 7976*, 79761Z (2011).

[12] Follador, M., Conn, A.T. and Rossiter, J. "Bistable minimum energy structures (BiMES) for binary robotics," *Smart Mater. Struct.*, 24(6) (2015).

[13] Choi, H.R., Jung, K., Ryew, S., Nam, J.-D., Jeon, J., Koo, J.C. and Tanie, K., "Biomimetic soft actuator: design, modeling, control, and applications," *IEEE/ASME Trans. Mech.* 10(5), 581 (2005).

[14] Nguyen, C.T., Phung, H., Nguyen, T.D., Jung, H. and Choi, H.R. " Multiple-degrees-of-freedom dielectric elastomer actuators for soft printable hexapod robot," *Sens. Actuators A Phys.*, 267, 505-516 (2017).

[15] Conn, A.T., Hinitt, A.D. and Wang, P., "Soft segmented inchworm robot with dielectric elastomer muscles," *Proc. SPIE 9056*, 90562L (2014).

[16] Cao, C., Burgess, S. and Conn, A.T., "Towards a dielectric elastomer resonator driven flapping wing micro air vehicle," *Frontiers in Robotics and AI*, 5, 137 (2019).

[17] Carpi, F., Frediani, G. and De Rossi, D., " Hydrostatically Coupled dielectric elastomer actuators," *IEEE/ASME Trans. Mech.*, 15(2) (2010).

[18] Cao, C., Gao, X. and Conn, A.T., "A compliantly-coupled double cone dielectric elastomer actuator using magnetic repulsion," *Appl. Phys. Lett.*, 114, 011904 (2019).

[19] Pei, Q., Rosenthal, M., Stanford, S., Prahlad, H. and Pelrine, R., "Multiple-degrees-of-freedom electro elastomer roll actuators," *Smart Mater. Struct.*, 13(5), N86 (2004).

[20] Cao, C. and Conn, A.T., "Performance optimization of a conical dielectric elastomer actuator," *Actuators*, 7(2), 32 (2018).